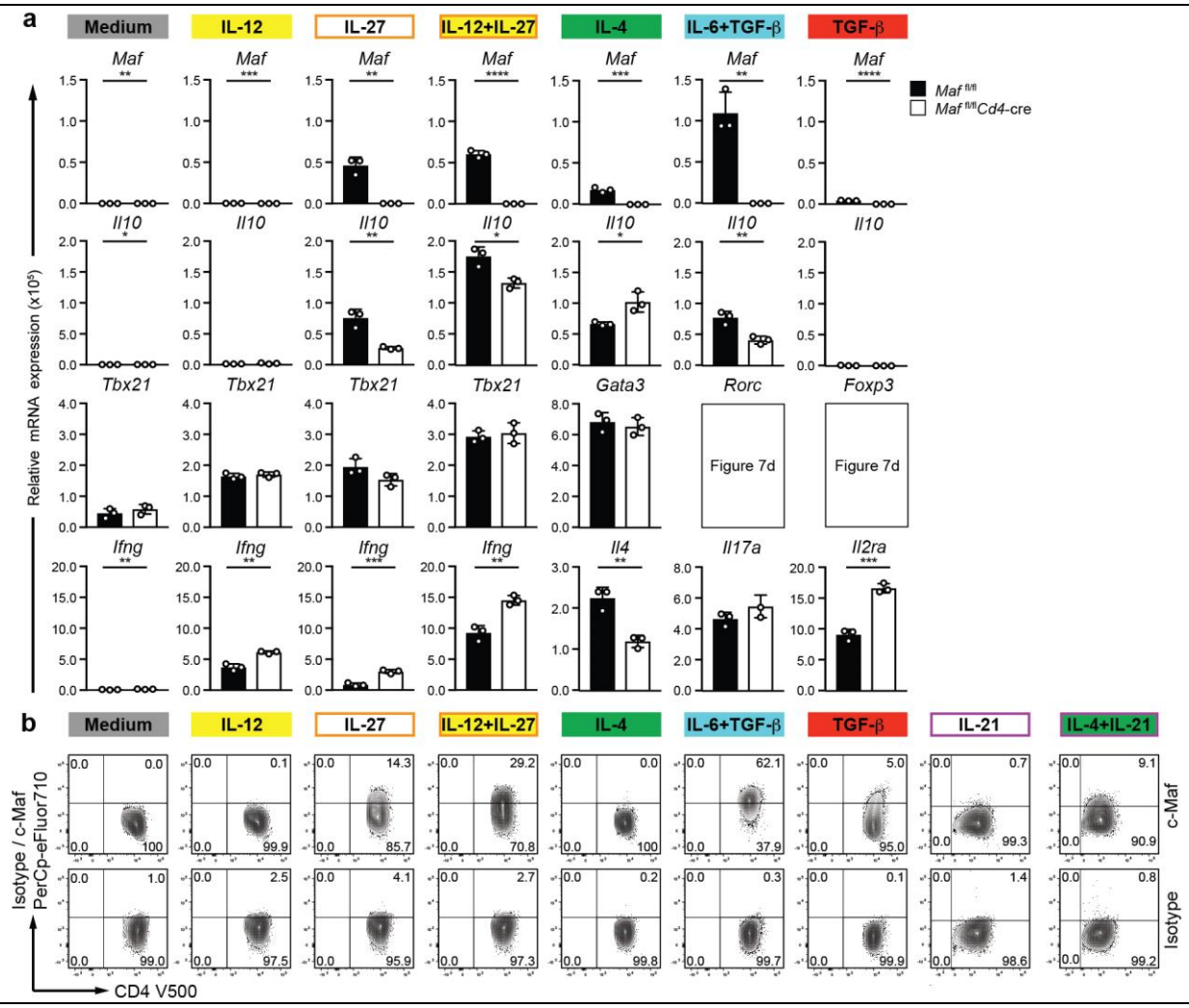

Supplementary Figure 1

The induction and effect of c-Maf on CD4⁺ T cell differentiation in vitro.

a, Naive CD4⁺ T cells from *Maf* $^{fl/fl}$ and *Maf* $^{fl/fl}$*Cd4*-cre were sorted and stimulated in vitro with anti-CD3 and anti-CD28 in the presence of medium alone, IL-12, IL-27, IL-12+IL-27, IL-4, TGF-β+IL-6 or TGF-β and assessed for the mRNA expression of *Maf*, *Il10* and master regulator transcription factors *Tbx21*, *Gata3*, *Rorc* and *Foxp3* and hallmark cytokines *Ifng*, *Il4* and *Il17a* as well as *Il2ra* relative to *Hprt* as follows. Medium, IL-12, IL-27, IL-12+IL-27: *Maf*, *Il10*, *Tbx21*, *Ifng* (day 3); IL-4: *Maf* (day 5), *Il10* (day 5), *Gata3* (day 4), *Il4* (day 5); TGF-β +IL-6: *Maf* (day 1), *Il10* (day 2), *Il17a* (day 5); TGF-β: *Maf*, *Il10*, *Foxp3*, *Il2ra* (day 3) (n=3 culture wells per condition, mean±SD; * $P < 0.05$, ** $P < 0.01$, *** $P < 0.001$, **** $P < 0.0001$, unpaired *t*-test, two-tailed). Representative data from three biological experiments are shown. **b**, Naive CD4⁺ T cells from wild-type mice were sorted, stimulated as in (a) and assessed for intracellular c-Maf on day 3. Depicted are dot plots of c-Maf versus isotype control gated on live CD4⁺ T cells. Representative data from two independent experiments are shown.

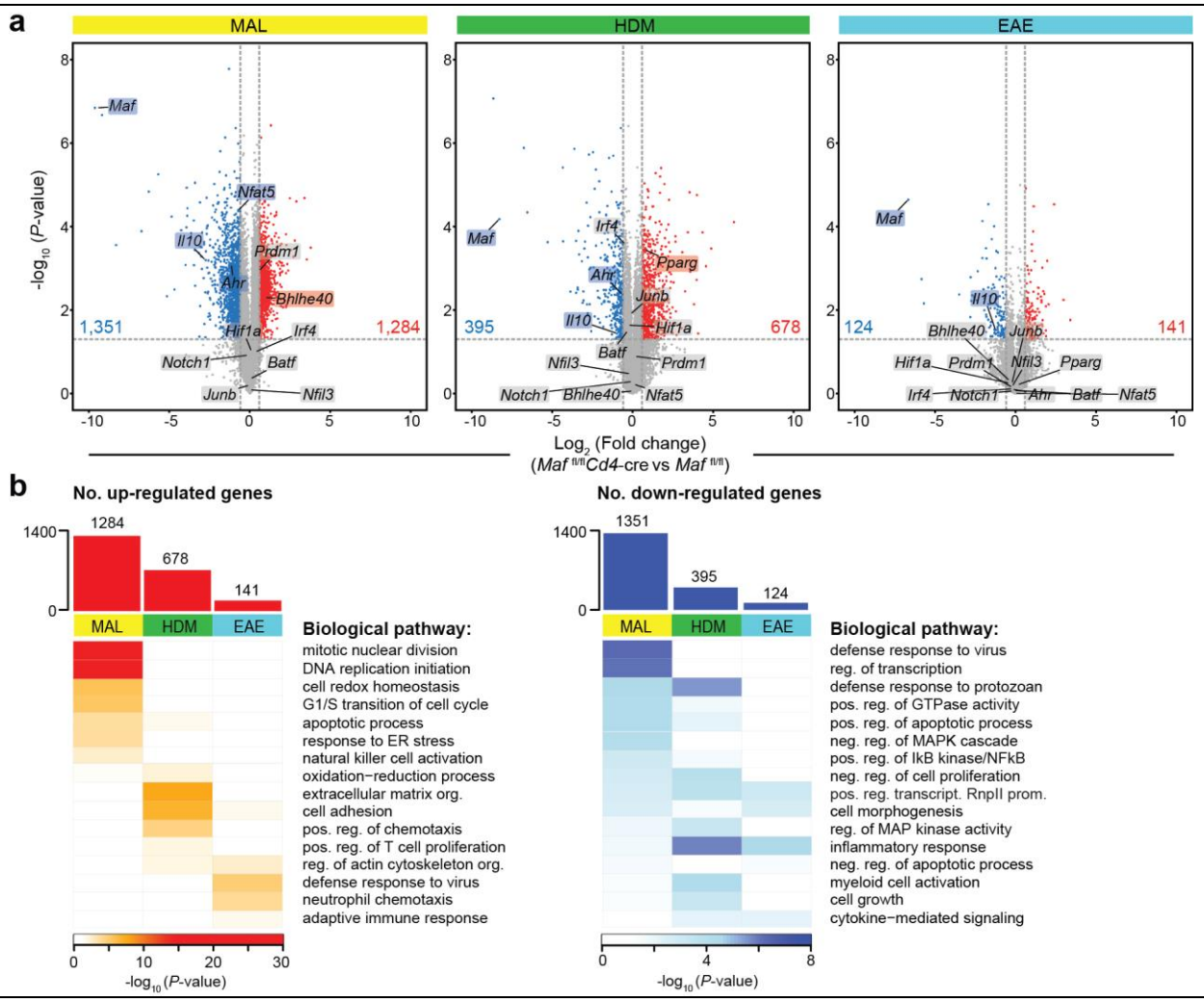

Supplementary Figure 2

Supporting information for differential gene expression analyses.

CD4⁺ T cells from malaria, HDM and EAE challenged *Maf*$^{fl/fl}$*Cd4*-cre vs *Maf*$^{fl/fl}$ mice were profiled by RNA-seq. **a**, Volcano plots of differentially expressed genes, with previously associated regulators of IL-10 depicted (blue, significantly down-regulated; red, significantly up-regulated; grey, non-differentially expressed) (n=3 independent animals (malaria) or biologically independent samples (HDM and EAE) per genotype; $P < 0.05$, absolute FC ≥ 1.5, moderated *t*-test, two-tailed). **b**, Manually curated list of top biological pathways as determined by GO enrichment analysis of each differentially up- and down-regulated genes in *Maf*$^{fl/fl}$*Cd4*-cre vs *Maf*$^{fl/fl}$ mice (n=3 independent animals (malaria) or biologically independent samples (HDM and EAE) per genotype).

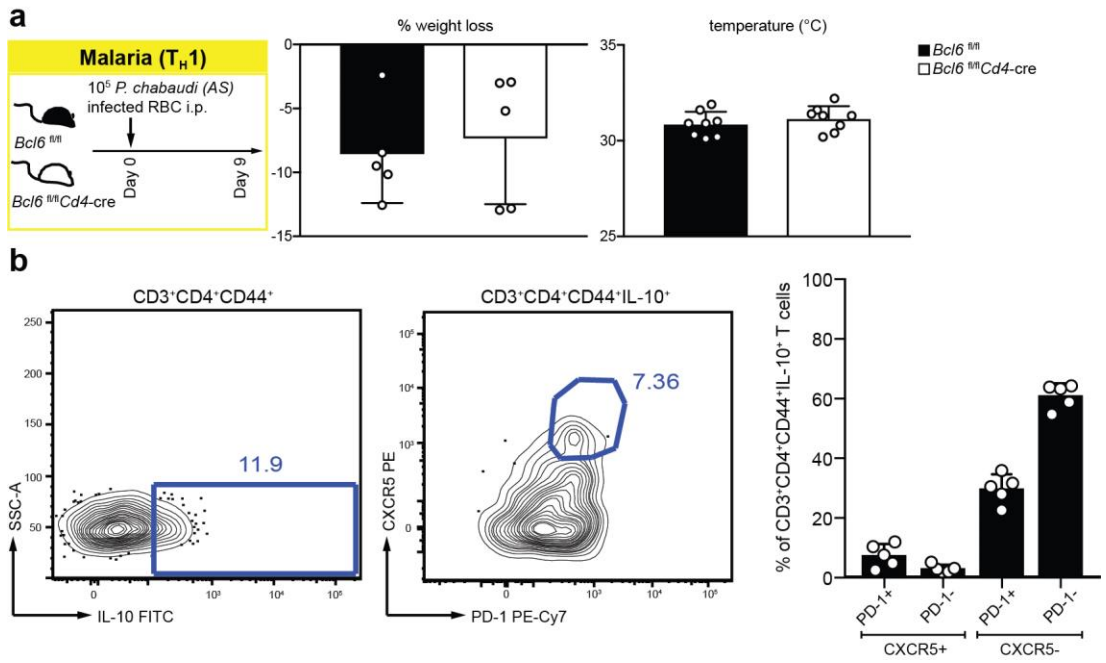

Supplementary Figure 3

Effect on pathology and phenotype of T_{FH} cells in acute phase of malaria.

a, Schematic of *P. chabaudi* infection in *Bcl6*$^{fl/fl}$ and *Bcl6*$^{fl/fl}$*Cd4*-cre mice, percentage weight loss (n=5, mean±SD) and temperature changes (n=8, mean±SD) on day 9 post *P. chabaudi* infection. Representative data from two biological experiments are shown. **b**, Representative cytokine staining of CD4$^+$ T cells on day 14 post *P. chabaudi* infection in C57BL/6J mice, plots are gated on live CD3$^+$CD4$^+$CD44$^+$ T cells. Pooled data from two biological experiments are shown (n=5, mean±SD).

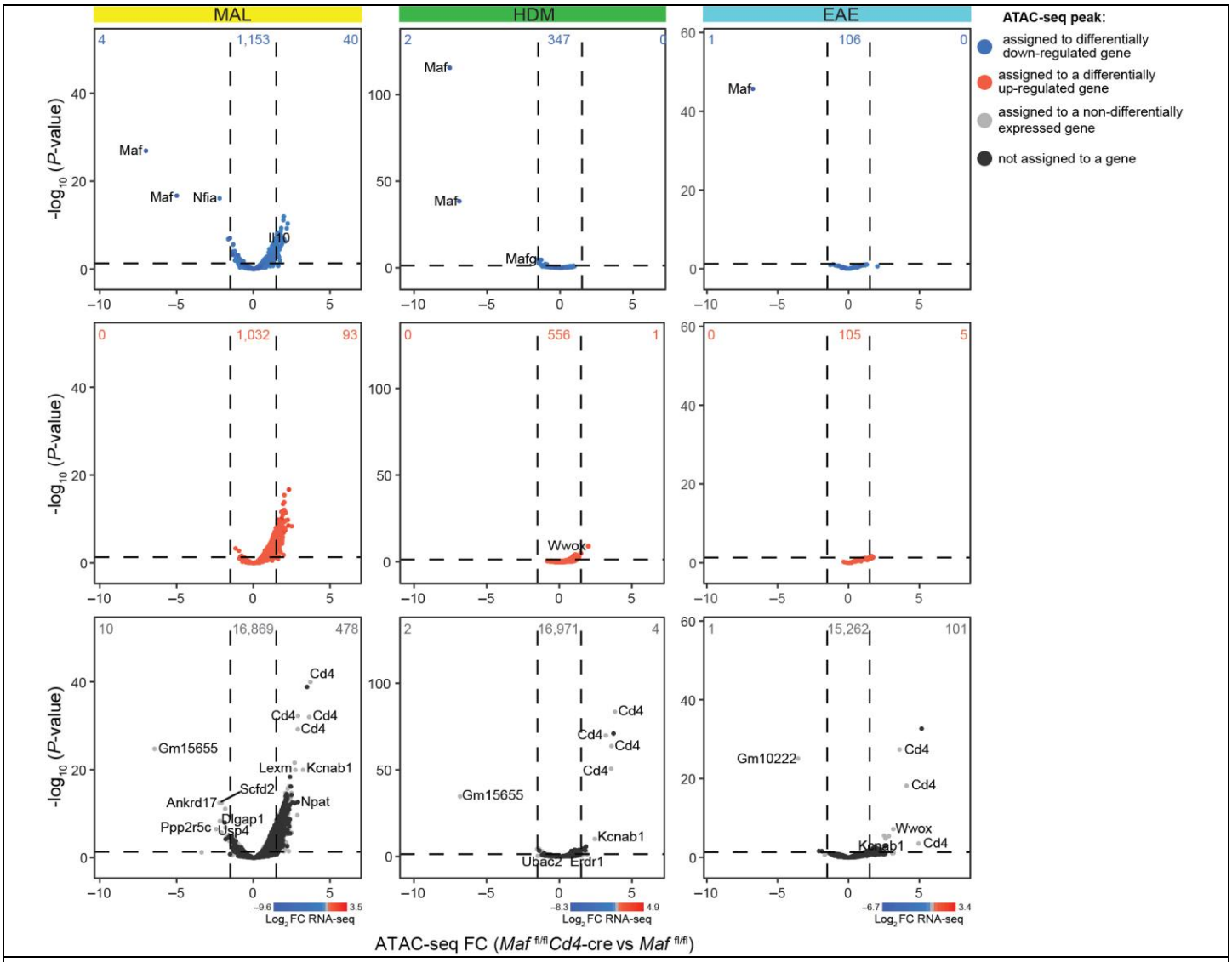

Supplementary Figure 4

Changes in chromatin accessibility do not account for transriptional disregulation in the absence of c-Maf.

Volcano plots of accessibility changes in ATAC-Seq consensus peak sets in CD4$^+$ T cells from malaria, HDM allergy and EAE challenged *Maf*$^{fl/fl}$*Cd4*-cre vs *Maf*$^{fl/fl}$ mice (n=3 independent animals (malaria) or biologically independent samples (HDM and EAE) per genotype, statistical significance called using DiffBind 2.02 with FDR < 0.05, absolute fold change ≥ 1.5) assigned to genes (see Supplementary Information for computational methods) and mapped to RNA-seq fold-change values. The top ten peaks ranked by fold-change were labeled with their assigned gene, as well as any remodeled peak assigned to *Il10*.

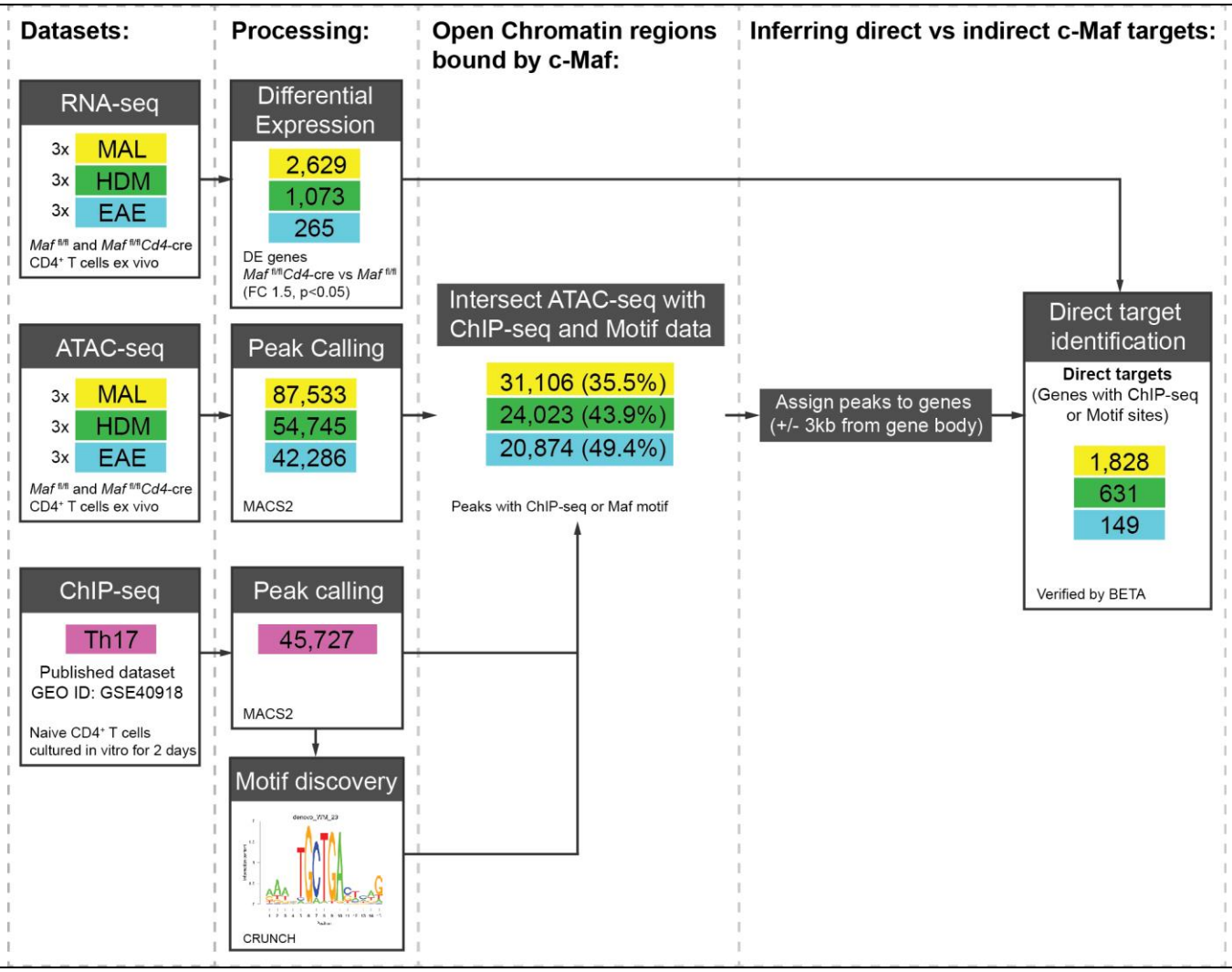

Supplementary Figure 5

Framework schematic for the identification of putative direct targets of c-Maf.

For each disease model, the c-Maf ChIP-seq (GSE40918) and motif datasets were filtered according to the accessibility as determined by ATAC-seq, allowing the identification of putative c-Maf binding sites and estimation of its relevance in explaining RNA-seq-defined transcriptional changes observed upon c-Maf deletion (see Supplementary Information for computational methods).

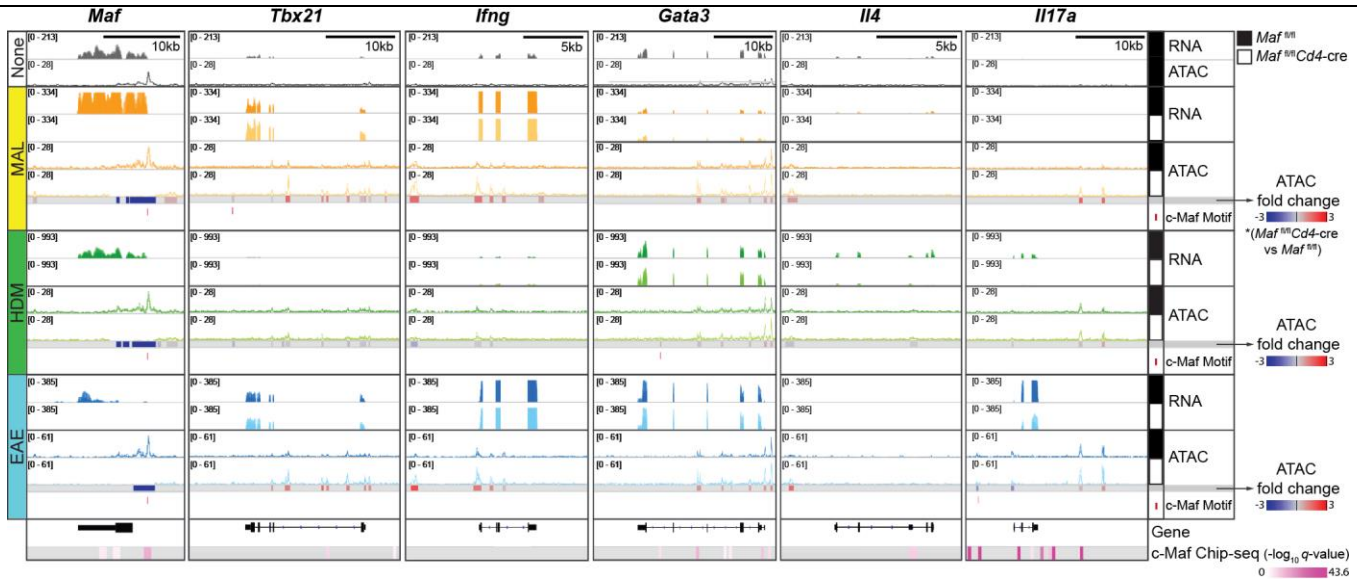

Supplementary Figure 6

Genome browser tracks of other key immune genes.

Genome browser tracks of read coverage of RNA-seq and ATAC-seq in CD4$^+$ T cells from the malaria, HDM allergy and EAE challenged *Maf*$^{fl/fl}$*Cd4*-cre vs *Maf*$^{fl/fl}$ mice (shown as an overlay of n=3 independent animals (malaria) or biologically independent samples (HDM and EAE) per genotype), as compared to untreated control and matched to c-Maf ChIP-seq (GSE40918) and motif sites.